

Dynamic signature of molecular association in methanol

C. E. Bertrand, J. L. Self, J. R. D. Copley, and A. Faraone

Citation: *The Journal of Chemical Physics* **145**, 014502 (2016); doi: 10.1063/1.4954964

View online: <http://dx.doi.org/10.1063/1.4954964>

View Table of Contents: <http://scitation.aip.org/content/aip/journal/jcp/145/1?ver=pdfcov>

Published by the [AIP Publishing](#)

Articles you may be interested in

[Molecular dynamics simulations of the structure and single-particle dynamics of mixtures of divalent salts and ionic liquids](#)

J. Chem. Phys. **143**, 124507 (2015); 10.1063/1.4931656

[Dynamics in molecular and molecular-ionic crystals: A combined experimental and molecular simulation study of reorientational motions in benzene, pyridinium iodide, and pyridinium nitrate](#)

J. Chem. Phys. **138**, 024508 (2013); 10.1063/1.4774096

[Molecular-dynamics simulations of dimethylsulfoxide-methanol mixtures](#)

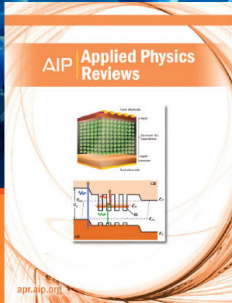
J. Chem. Phys. **123**, 154507 (2005); 10.1063/1.2085052

[Molecular association between water and dimethyl sulfoxide in solution: A molecular dynamics simulation study](#)

J. Chem. Phys. **110**, 6412 (1999); 10.1063/1.478544

[A molecular Ornstein–Zernike study of popular models for water and methanol](#)

J. Chem. Phys. **110**, 1138 (1999); 10.1063/1.478171



NEW Special Topic Sections

NOW ONLINE
Lithium Niobate Properties and Applications:
Reviews of Emerging Trends

AIP | Applied Physics
Reviews

Dynamic signature of molecular association in methanol

C. E. Bertrand,¹ J. L. Self,² J. R. D. Copley,¹ and A. Faraone^{1,a)}

¹*NIST Center for Neutron Research, National Institute of Standards and Technology, Gaithersburg, Maryland 20899, USA*

²*McKetta Department of Chemical Engineering, University of Texas, Austin, Texas 78712, USA*

(Received 30 March 2016; accepted 14 June 2016; published online 5 July 2016)

Quasielastic neutron scattering measurements and molecular dynamics simulations were combined to investigate the collective dynamics of deuterated methanol, CD₃OD. In the experimentally determined dynamic structure factor, a slow, non-Fickian mode was observed in addition to the standard density-fluctuation heat mode. The simulation results indicate that the slow dynamical process originates from the hydrogen bonding of methanol molecules. The qualitative behavior of this mode is similar to the previously observed α -relaxation in supercooled water [M. C. Bellissent-Funel *et al.*, Phys. Rev. Lett. **85**, 3644 (2000)] which also originates from the formation and dissolution of hydrogen-bonded associates (supramolecular clusters). In methanol, however, this mode is distinguishable well above the freezing transition. This finding indicates that an emergent slow mode is not unique to supercooled water, but may instead be a general feature of hydrogen-bonding liquids and associating molecular liquids. [<http://dx.doi.org/10.1063/1.4954964>]

I. INTRODUCTION

As the simplest monohydroxy alcohol, methanol serves as a model system for understanding the generic properties of alcohols and, more generally, hydrogen-bonding liquids. Because the hydroxyl hydrogen is a hydrogen bond donor and the oxygen atom is a hydrogen bond acceptor, methanol molecules form quasi one-dimensional, string-like associates, i.e. contiguous sets of hydrogen-bonded molecules. The presence of these associates strongly affects the properties of the liquid. Thermodynamic and structural properties of methanol have been studied extensively,¹ whereas the collective dynamics have not been investigated thoroughly. The characterization of these dynamics is important for understanding both the molecular origins of macroscopic transport properties and methanol's glass forming ability.

The collective dynamics of methanol can be contrasted with those of a simple liquid, such as argon. The relaxation of density correlations in a simple liquid is well described by a diffusive collective heat mode and two propagating sound modes.² Over molecular length scales, these modes are strongly affected by the structure of the fluid.³ For example, the relaxation rate of the heat mode exhibits a de Gennes narrowing, i.e. a minimum over length scales corresponding to the main structure factor peak. A general understanding of how these collective modes are altered in the presence of extended associates does not exist.

Recently, the static and dynamic properties of associates in colloids,⁴ protein solutions,⁵ and ionic liquids^{6,7} have attracted increasing attention. It is still debated which of the observed features in these systems constitute a definitive signature of associating behavior.⁸ A general framework, with inputs from the mode-coupling theory (MCT) of the kinetic glass transition, has been developed to model the behavior of

colloidal particles with specific types of isotropic interaction potentials.⁹ Remarkably, a similar understanding is missing for many extensively studied associating molecular liquids.

There is some evidence that the formation of hydrogen-bonded associates does lead to emergent dynamic phenomena in molecular liquids, as well. A slow relaxation mode was observed in the collective dynamics of supercooled water by Sciortino *et al.*¹⁰ via molecular dynamics (MD) simulations. This mode was found in addition to the heat mode¹¹ and was dubbed the α -relaxation in analogy with concept from the MCT. Within this framework, the α -relaxation was interpreted as resulting from caging effects and the slow relaxation of water's tetrahedral hydrogen-bond network. Subsequent neutron spin-echo spectroscopy measurements confirmed the existence of this α -relaxation experimentally.¹²

In this paper, we report the observation of a slow, non-Fickian mode in the collective dynamics of fully deuterated methanol from combined quasielastic neutron scattering (QENS) measurements and molecular dynamics (MD) simulations. This mode is similar in many regards to the α -relaxation observed in supercooled water. The appearance of a long-time decay is often associated with glassy behavior in supercooled liquids. In stark contrast, the slow mode in methanol was observed far above the freezing point ($T_M = 176$ K).

As will be shown subsequently, the observed slow mode is fundamentally collective in nature and is therefore absent from the single particle dynamics most commonly investigated in QENS studies of protonated methanol. However, it is observable in the QENS spectra of fully deuterated methanol, where the incoherent scattering from the hydrogen atoms is minimized. For this reason, we have focused exclusively on fully deuterated methanol.

Even though QENS is well suited to probe the length and time scales associated with the molecular dynamics of methanol,¹³ the unambiguous interpretation of QENS

^{a)}Electronic mail: afaraone@nist.gov

data is complicated by a limited energy resolution, the size of the accessible energy window, and the presence of both incoherent and coherent scattering contributions. Consequently, complimentary MD simulations are essential in this case for the accurate interpretation of the QENS data.

II. EXPERIMENTS AND MD SIMULATIONS

Fully deuterated methanol (CD_3OD , D 99.8% purity) was purchased from Sigma-Aldrich¹⁴ and used without further purification. Quasielastic neutron scattering (QENS) measurements were made using the Disk Chopper Spectrometer (DCS) on NG-4¹⁵ at the NIST Center for Neutron Research. Multiple scattering was largely suppressed using an annular sample geometry with radial thickness of 0.08 mm which results in better than 90% transmission. Measurements were performed at a neutron wavelength of $\lambda = 0.5$ nm. In this configuration, the DCS instrumental energy resolution is approximately Gaussian with a full width at half maximum of roughly 100 μeV . A standard vanadium sample was used to determine detector efficiency and instrumental energy resolution. Data were reduced and corrected for scattering from the sample container to obtain constant Q spectra, using routines available in the DAVE software package.¹⁶ The sample temperature was controlled using a closed cycle refrigerator with an accuracy of roughly 1 K.

The experimental QENS spectra were modeled at the atomic level using data from molecular dynamics simulations. These simulations were performed with Gromacs 4.6.3¹⁷ using the leap frog integrator and a 2 fs time step. The OPLS-AA¹⁸ force field was used to model (protiated) methanol. The simulations were performed in the NPT ensemble ($P = 100$ kPa = 1 bar) using a Nosé-Hoover thermostat ($\tau_T = 0.5$ ps) and a Parrinello-Rahman barostat ($\tau_P = 2.5$ ps). The periodic simulation box contained $N = 2048$ molecules. Lennard-Jones and Coulomb interactions were truncated at 1.1 nm and the Particle-Mesh Ewald method was used to account for long-range electrostatic interactions. The system was equilibrated for 5 ns at each condition and data were collected for an additional 5 ns. Experimentally accessible correlation functions were calculated using the scattering cross section of deuterium rather than hydrogen.

III. NEUTRON SCATTERING THEORY

Scattering theory in multi-atom systems is often presented in terms of particle-number normalized correlation functions. In this section, we instead express scattering quantities in terms of volume normalized correlation functions in order to simplify the presentation and analysis.

The collective dynamic correlations between atomic species α and β in the volume V are characterized by the atomic full intermediate scattering function,

$$F^{\alpha\beta}(Q, t) = \frac{1}{V} \left\langle \sum_{i,j} e^{i\mathbf{Q} \cdot [\mathbf{R}_i^\alpha(t) - \mathbf{R}_j^\beta(0)]} \right\rangle, \quad (1)$$

where $\mathbf{R}_i^\alpha(t)$ is the position of the i th atom of species α at time t and the magnitude of the wavevector $Q = |\mathbf{Q}|$ determines the

inverse length-scale probed. In the above expression, the angle brackets indicate an ensemble average. Similarly, the atomic self intermediate scattering function, which characterizes the self dynamic correlations of species α , is given by

$$F^\alpha(Q, t) = \frac{1}{V} \left\langle \sum_j e^{i\mathbf{Q} \cdot [\mathbf{R}_j^\alpha(t) - \mathbf{R}_j^\alpha(0)]} \right\rangle. \quad (2)$$

The intermediate scattering functions are readily calculated from MD trajectories.¹⁹

The double differential cross section measured by QENS can be expressed as the sum of a coherent term and an incoherent term,

$$S(Q, E) = S^{\text{coh}}(Q, E) + S^{\text{inc}}(Q, E), \quad (3)$$

where the magnitude of the wavevector and energy transfer, $Q = |\mathbf{k}_i - \mathbf{k}_f|$ and $E = E_i - E_f$, respectively, are defined by the differences between the initial and final wavevectors, \mathbf{k}_i and \mathbf{k}_f , and energies, E_i and E_f , of a scattered neutron.¹³ The coherent dynamic structure factor is a weighted sum of atomic dynamic structure factors,

$$S^{\text{coh}}(Q, E) = \sum_{\alpha, \beta} b_\alpha^{\text{coh}} b_\beta^{\text{coh}} S^{\alpha\beta}(Q, E), \quad (4)$$

where b_α^{coh} is the coherent neutron scattering length of atomic species α . $S^{\text{coh}}(Q, E)$ reflects the collective dynamics of the system and is comprised of both self and distinct parts. If the three hydrogen atoms of the methyl group are treated as being equivalent, ten distinct terms contribute to the sum in Eq. (4). Many QENS experiments have focused solely on the incoherent dynamics of methanol, due to the inherent complexity of modeling $S^{\text{coh}}(Q, E)$.

The incoherent dynamic structure factor is a weighted sum of the self parts of the atomic dynamic structure factors,

$$S^{\text{inc}}(Q, E) = \sum_\alpha b_\alpha^{\text{inc}} b_\alpha^{\text{inc}} S^\alpha(Q, E), \quad (5)$$

where b_α^{inc} is the incoherent neutron scattering length of atomic species α .

The dynamic structure factors and intermediate scattering functions are related to each other via a time Fourier transform,

$$S^x(Q, E) = \frac{1}{2\pi} \int_{-\infty}^{\infty} dt e^{-i(E/\hbar)t} F^x(Q, t), \quad (6)$$

where x stands for any of the aforementioned superscripts, e.g. coh or $\alpha\beta$. For brevity, the time Fourier transform can be denoted by \mathcal{F} , i.e., $S^x(Q, E) = \mathcal{F} \{F^x(Q, t)\}$. In the same fashion, the inverse transform can be used to define the intermediate scattering functions,

$$F^x(Q, t) = \mathcal{F}^{-1} \{S^x(Q, E)\}. \quad (7)$$

In a static neutron scattering experiment, data are collected without analyzing the energy transfer. Hence, static structure factors can be obtained by integrating dynamic structure factors over all E . For example, the coherent structure factor is given by

$$S^{\text{coh}}(Q) = \int_{-\infty}^{\infty} dE S^{\text{coh}}(Q, E) = F^{\text{coh}}(Q, t = 0). \quad (8)$$

The last term in the above expression, $F^{\text{coh}}(Q, t = 0)$, was used to calculate $S^{\text{coh}}(Q)$ from the MD simulations.

That the self correlations, and therefore the incoherent scattering, do not contain any structural information is a direct consequence of the identity,

$$S^{\alpha}(Q) = F^{\alpha}(Q, t = 0) = \frac{N^{\alpha}}{V}, \quad (9)$$

where N^{α} is the number of atoms of species α .

IV. RESULTS AND DISCUSSION

Measured scattering intensities, at momentum transfer Q and energy transfer E , were analyzed with the following phenomenological model:

$$I(Q, E) = \mathcal{F} \{ A e^{-\Gamma t} \} \otimes R(Q, E) + B, \quad (10)$$

where \mathcal{F} denotes a time Fourier transform, \otimes is the convolution operator, and $R(Q, E)$ is the instrumental resolution function. In the above expression, A is an amplitude, Γ is the long-time decay rate, and B is a background constant. The inclusion of B is an approximate means of accounting for short-time (roughly sub-picosecond) dynamic processes that lie beyond the ± 1 meV energy window employed here. Representative QENS spectra and fit curves are presented in Fig. 1. Discussion of the extracted fit parameters will be deferred until the corresponding MD results have been introduced.

The coherent and incoherent structure factors calculated from our MD simulations are presented in Fig. 2. The coherent structure factor exhibits a single pronounced peak at $Q_{\text{max}} \approx 17 \text{ nm}^{-1}$. This result is in agreement with previous measurements.²⁰ We note that the structure of liquid methanol has been extensively investigated in the past using X-rays^{21,22} and neutron diffraction with deuterium substitution.^{23–25} For fully deuterated methanol, the value of the incoherent structure factor, which is Q -independent, is much smaller than the coherent structure factor, except at low Q , where they become comparable. The coherent structure of the liquid does not change qualitatively with decreasing temperature, despite an increasing degree of association, i.e. hydrogen bonding.

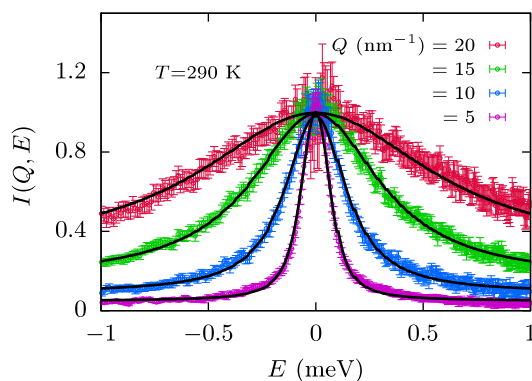


FIG. 1. Representative QENS spectra for CD_3OD . The points are experimental data and the continuous lines are fits corresponding to Eq. (10). The width of the spectra is proportional to the decay rate Γ . The spectra have been normalized to emphasize the dependence of Γ on Q . Error bars represent one standard deviation.

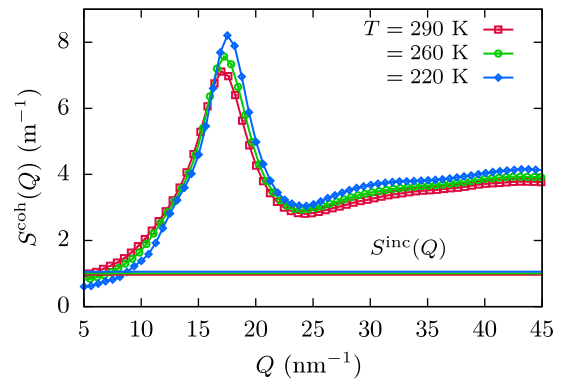


FIG. 2. The coherent static structure factor, $S^{\text{coh}}(Q)$ of CD_3OD , at three different temperatures. The incoherent structure factor S^{inc} (horizontal line) is shown at the same temperatures for comparison. Both S^{inc} and the large Q limit of S^{coh} vary with temperature through their dependence on the volume V .

The intermediate scattering functions, $F(Q, t)$, corresponding to the experimental scattering intensities were calculated from the MD simulations by taking appropriately weighted sums of the atomic intermediate scattering functions. Representative intermediate scattering functions are presented in Fig. 3. Qualitatively, two dynamic modes are observed. As a result, the decay was modeled as a sum of two exponentials, specifically,

$$F(Q, t) = S(Q) [(1 - x) e^{-zt} + x e^{-\Gamma t}], \quad (11)$$

where $S(Q)$ is the neutron-scattering structure factor (comprised of both coherent and incoherent contributions), z is the short-time decay rate, Γ is the long-time decay rate, and x determines the relative weight of the two modes. Examples of fits are also shown in Fig. 3. With the assignments $A = xS(Q)$ and $B = (1 - x)S(Q)/\pi z$, the QENS and MD models given by Eqs. (10) and (11) are equivalent in the limit $E \ll \hbar z$. We note that both fit models neglect the effects of propagating acoustic modes. This approximation is justifiable over the experimental Q range, where distinct Brillouin peaks are not distinguishable. However, use of this approximation implies that short-time ballistic behavior is not accurately

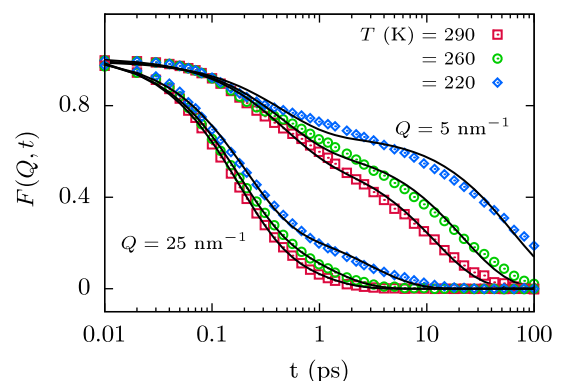


FIG. 3. Representative intermediate scattering functions for CD_3OD calculated from MD simulations. The functions have been normalized to $S(Q)$ in order to emphasize the dependence of the long-time decay on T . The continuous lines are fits corresponding to Eq. (11). At low Q , two decay modes are clearly distinguishable.

represented. This consideration does not significantly impact on our findings, which are primarily concerned with the long-time behavior.

Equation (11) is similar in spirit to the model used by Liao *et al.*¹¹ for their analysis of the α -relaxation in supercooled water. These authors employed a parameter-free model of the heat mode based on generalized hydrodynamics and a stretched exponential for the long-time decay. In our case, the addition of a stretching exponent does improve the fit quality, but also leads to spurious correlations, since both z and Γ are unconstrained in our model. Furthermore, under the conditions studied, the long-time decay in methanol is not nearly as stretched as it is in supercooled water.

The quality of the fits is sufficient for both the QENS spectra and MD scattering functions in light of the simplicity of the models employed. Given the inherent complexity of the scattering functions, any reasonable fit model is necessarily phenomenological in nature. Some systematic deviations due to the choice of model are apparent, especially at low Q , but the qualitative behavior is well captured. Previous QENS data from CD₃OD²⁶ were analyzed with a complex model comprised of five exponential functions accounting for both coherent and incoherent contributions as well as distinct translational and rotational contributions. We have found our simplified model to be entirely adequate for the present purpose.

The Q dependence of the extracted long-time decay rates is reported in Fig. 4. These data are the central result of this work. In what follows, it will be demonstrated that Γ represents a slow, collective, non-Fickian mode related to the formation of extended associates in methanol. The mere existence of this mode constitutes a unique dynamic signature of association. The MD and QENS results for Γ are generally in agreement, particularly at $T = 260$ K. This agreement validates, *a posteriori*, the appropriateness of the simulation and analysis methods. At the lowest temperature, $T = 220$ K, values of Γ appear to differ by a constant scale factor. This may stem from the particular parametrization of hydrogen bonding employed by the OPLS-AA model. The MD values of Γ appear to dip at high Q for $T = 290$ K. If the values of x are fixed to those extracted from the fits at 260 K, the resulting

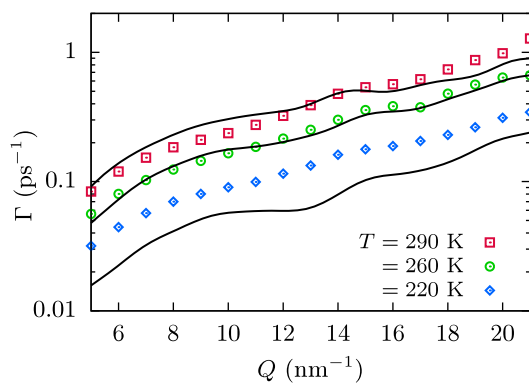


FIG. 4. The decay rate Γ as a function of Q extracted from fits of the experimental (points) and simulation (continuous line) data. Error bars are contained within the size of the experimental points. The Q and T dependence of Γ appear to be decoupled.

values of Γ fall within the error bars for all experimental points in this Q range. Hence, these deviations are likely induced by the proximity of z and Γ at these conditions and the inability of the fit model to fully resolve the difference between them.

The Q and T dependences of Γ appear to be decoupled in Fig. 4. The temperature dependence of Γ can be described by the Arrhenius law for activated dynamic processes,

$$\Gamma \propto \exp\left(-\frac{E_a}{k_B T}\right), \quad (12)$$

where E_a is the activation energy and k_B is Boltzmann's constant. When applied to the extracted values of Γ , Eq. (12) yields average activation energies of $E_a^{\text{QENS}} \simeq 80$ meV and $E_a^{\text{MD}} \simeq 130$ meV. These values both fall within the range of energies for hydrogen bond formation. This observation supports an interpretation of the slow mode as resulting from the dissolution and formation of methanol associates.

It is not immediately obvious that Γ reflects the collective dynamics of the system since the scattering functions contain both coherent and incoherent terms. The coherent term corresponds to collective dynamics, whereas the incoherent term corresponds to self dynamics. This ambiguity is resolved by studying the behavior of each term separately. Decay rates extracted from fits of calculated coherent (coh) and incoherent (inc) intermediate scattering functions are plotted in Fig. 5(a). The coherent function was fitted using Eq. (11) with decay rates z^{coh} and Γ^{coh} , whereas the incoherent function was fitted using a single exponential function with decay rate z^{inc} . The relative amplitudes of the coherent and incoherent terms are determined by their respective structure factors, $S^{\text{coh}}(Q)$ and $S^{\text{inc}}(Q)$. At low Q , the values of $S^{\text{coh}}(Q)$ and $S^{\text{inc}}(Q)$ are comparable, and Γ reflects z^{inc} and the slow self dynamics. As Q approaches Q_{max} , $S^{\text{coh}}(Q)$ becomes significantly larger than $S^{\text{inc}}(Q)$ and Γ increasingly reflects Γ^{coh} and the collective dynamics. Lastly, as expected for a heat mode, z and z^{coh}

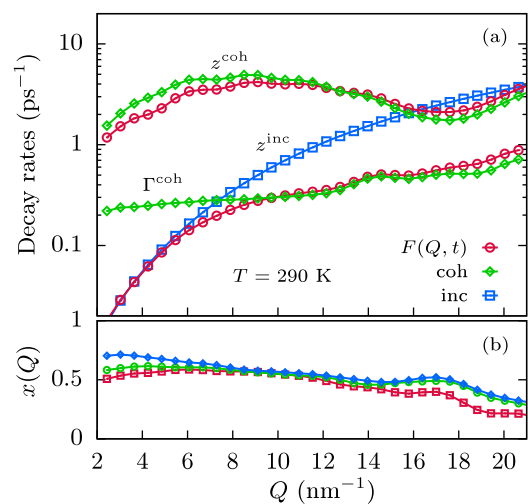


FIG. 5. (a) Comparison of decay rates extracted from the total, coherent, and incoherent intermediate scattering functions. The long-time decay rate Γ is strongly affected by incoherent scattering at low Q , but primarily reflects coherent scattering in the experimental Q range. (b) Relative weight of the slow mode decreases with increasing Q , indicating that the slow mode is most prominent over larger length scales.

oscillate around $z^{\text{inc}} \simeq D_s Q^2$ at high Q . We note that the extracted value of z is relatively unaffected by the incoherent scattering, since z and z^{coh} are similar over the entire Q range. To summarize, the slow mode associated with Γ does in fact represent the collective (coherent) dynamics over the majority of the experimental Q range.

The preceding discussion illustrates why the slow mode was not emphasized for the previous QENS measurements of CD_3OD made by Bermejo *et al.*²⁶ The decay rates reported by these authors at 250 K are very similar to the values of Γ reported here at 260 K. In the analysis of these decay rates of Bermejo *et al.*, high Q data were excluded because they deviated from the Fickian Q^2 behavior observed at low Q . In hindsight, with the support of the MD simulation results, it seems likely that the results reported by these authors actually reflect z^{inc} and the self dynamics observed at low Q .

The relative weight of the slow mode, as parametrized by x , is shown in Fig. 5(b). We note that in the work of Liao *et al.*,¹¹ the behavior of their ‘‘collective Debye-Waller factor’’ $A(Q)$ is similar to that of x . In particular, $A(Q)$ was found to be weakly temperature dependent and to decrease with increasing Q .

Values of z extracted from the fits of $F(Q, t)$ at $T = 290$ K are shown in Fig. 5(a). Values at other temperatures behave similarly. An in-depth look at the Q -dependence of z further allows it to be identified with the heat mode found in simple liquids. In the hydrodynamic limit ($Q \rightarrow 0$), the relaxation rate of the heat mode is $z = D_T Q^2$, where D_T is the thermal diffusion coefficient. However, this relationship breaks down over molecular length scales. In dense atomic liquids, for Q values not too small, the heat mode decay rate is well-described by the hard-sphere result,²⁷

$$z = \frac{D_s Q^2}{S(Q)} d(Q), \quad (13)$$

where D_s is the self-diffusion coefficient, $S(Q)$ is the atomic structure factor, and $d(Q)$ is the so-called velocity transfer function. Equation (13) has two important consequences. First, the inverse dependence of z on $S(Q)$ leads to a minimum in the vicinity of the structure factor maximum at Q_{max} . This phenomenon is clearly visible in Fig. 5(a) near $Q_{\text{max}} \simeq 17 \text{ nm}^{-1}$, the location of the methanol structure factor peak. Second, at Q greater than Q_{max} , z oscillates around $D_s Q^2$, since $S(Q) \rightarrow 1$ and $d(Q) \rightarrow 1$ as $Q \rightarrow \infty$. This behavior is also observed in Fig. 5(a) and will be discussed further in the following paragraph. We note that, in contrast to z , the slow mode corresponding to Γ is relatively insensitive to the liquid structure.

Figure 6 displays the extracted decay rates for the center of mass motion. Using the thermal diffusivity, D_T , measured by photon correlation spectroscopy,²⁸ a naive extrapolation of the hydrodynamic heat-mode, $z = D_T Q^2$, to high Q gives the results shown in Fig. 6. Clearly this description of the heat mode deviates from the observed behavior over the experimental Q range. Using generalized hydrodynamics, Kirkpatrick has presented an analytic theory for the heat mode,²⁹ $z_{\text{H}}(Q)$, of a dense hard-sphere liquid that is applicable over the experimental Q range. This theory requires the hard-sphere structure factor as input, which

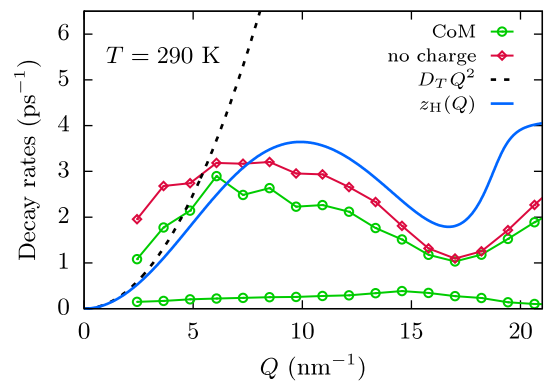


FIG. 6. Comparison of decay rates for the center of mass motion, with and without electric charge. The theoretical curves for the hydrodynamic (dashed) and hard-sphere (solid) theories are explained in the text.

we have calculated using the Percus-Yevick approximation,² where the hard-sphere diameter of methanol was estimated using $\sigma \simeq 2\pi/Q_{\text{max}} = 0.4 \text{ nm}$. Unlike Eq. (13), Kirkpatrick’s expression for $z_{\text{H}}(Q)$ has the correct low Q limit, but starts to break down for $Q > Q_{\text{max}}$. Notably, at low Q , the hydrodynamic and hard-sphere results approach each other as expected. While it is not surprising that the values of z extracted from our simulations do not match the hard-sphere theory exactly, they are remarkably similar. This comparison greatly strengthens the identification of z as the heat mode in the system.

The connection between the slow mode and the formation of hydrogen-bonded associates is highlighted by considering a model MD system in which electric charge has been set to zero. Molecules in this charge-free system only interact via the Lennard-Jones portion of the OPLS-AA potential. In this system, the intermediate scattering function for the center of mass (CoM) exhibits a single decay mode corresponding to the heat mode without any evidence of the slow mode corresponding to Γ . As seen in Figure 6, the decay rate of this heat mode is qualitatively identical to that observed in the unperturbed (charged) system. The absence of a slow collective mode in the charge-free system provides conclusive evidence that the observed mode can be attributed to hydrogen bonding and the formation of methanol associates. Additionally, both modes corresponding to z and Γ are observed for the CoM intermediate scattering function in the unperturbed system. This finding indicates that the slow mode is not connected with molecular rotations.

The methanol collective dynamics reported here are qualitatively similar to those observed by Zaccarelli *et al.*⁴ in simulations of a restricted-valence model of gel formation. In this work, an additional slow mode was observed at Q values below the structure factor peak and the corresponding relaxation rate was also found to decrease strongly with decreasing temperature. The mode was interpreted as resulting from the slow relaxation of the gel-network with the characteristic time scale set by the average lifetime of the gel-bonds. Given the strong analogies between the structure and dynamics of liquids and colloids,²⁷ it seems likely that the dynamic phenomena observed in hydrogen bonding liquids would also be present in systems of patchy, and other network forming, colloids.

The short-time, center of mass dynamics of molecular liquids appear to be reasonably approximated by the corresponding hard-sphere results with an appropriate choice of the hard-sphere diameter. In contrast, at present, a theory to explain the long-time, non-Fickian relaxation identified in this paper has not been developed. A careful modeling of the associative interactions (H-bonding in this case) would be required for this task. In principle, the MD trajectories contain all of the information required to accomplish this; in practice, such an effort would require the development of a new theoretical framework that is beyond the scope of the present investigation. Unfortunately, a more thorough understanding of the observed slow mode must be left for future work.

V. CONCLUSIONS

In summary, we have identified a novel slow mode in the collective dynamics of liquid methanol through a combination of quasielastic neutron scattering measurements and molecular dynamics simulations. This mode is a dynamic manifestation of the formation of extended methanol associates and exists in addition to the heat mode found in simple liquids. An Arrhenius law with an activation energy comparable to the energy of hydrogen bond formation describes the strong temperature dependence of this mode. The mode is similar to the α -relaxation observed in supercooled water, but it is observable under ambient conditions, far from the freezing point. Given the emphasis often placed on water's tetrahedral hydrogen bond network, it is important to emphasize that methanol molecules form quasi-linear associates and not a system spanning network. Taken together, these findings indicate that an emergent slow mode might be a generic feature of, at least, a significant subset of hydrogen-bonding liquids. Such a scenario is compatible with recent neutron scattering measurements of the dynamics in *m*-toluidine³⁰ and 1-propanol.³¹ Furthermore, coherent QENS data from other hydrogen-bonding molecular systems may need to be reassessed in light of these results.

ACKNOWLEDGMENTS

The authors would like to thank J. Teixeira for a critical reading of this manuscript. This work utilized facilities supported in part by the National Science Foundation under Agreement No. DMR-1508249. During the execution of this work JS was supported by the National Science

Foundation under Agreement No. DMR-0944772 as a Summer Undergraduate Research Fellow.

- ¹R. Böhmer, C. Gainaru, and R. Richert, *Phys. Rep.* **545**, 125 (2014).
- ²J. P. Hansen and I. R. McDonald, *Theory of Simple Liquids*, 3rd ed. (Academic Press, 2005).
- ³J. P. Boon and S. Yip, *Molecular Hydrodynamics* (Dover Publications, Mineola, NY, 1992).
- ⁴E. Zaccarelli, S. V. Buldyrev, E. La Nave, A. J. Moreno, I. Saika-Voivod, F. Sciortino, and P. Tartaglia, *Phys. Rev. Lett.* **94**, 218301 (2005).
- ⁵L. Porcar, P. Falus, W.-R. Chen, A. Faraone, E. Fratini, K. Hong, P. Baglioni, and Y. Liu, *J. Phys. Chem. Lett.* **1**, 126 (2010).
- ⁶M. Kofu, M. Nagao, T. Ueki, Y. Kitazawa, Y. Nakamura, S. Sawamura, M. Watanabe, and O. Yamamuro, *J. Phys. Chem. B* **117**, 2773 (2013).
- ⁷O. Yamamuro, T. Yamada, M. Kofu, M. Nakakoshi, and M. Nagao, *J. Chem. Phys.* **135**, 054508 (2011).
- ⁸Y. Liu, L. Porcar, J. Chen, W.-R. Chen, P. Falus, A. Faraone, E. Fratini, K. Hong, and P. Baglioni, *J. Phys. Chem. B* **115**, 7238 (2011).
- ⁹E. Zaccarelli, *J. Phys.: Condens. Matter* **19**, 323101 (2007).
- ¹⁰F. Sciortino, L. Fabbian, S.-H. Chen, and P. Tartaglia, *Phys. Rev. E* **56**, 5397 (1997).
- ¹¹C. Y. Liao, F. Sciortino, and S. H. Chen, *Phys. Rev. E* **60**, 6776 (1999).
- ¹²M. C. Bellissent-Funel, S. Longeville, J. M. Zanotti, and S. H. Chen, *Phys. Rev. Lett.* **85**, 3644 (2000).
- ¹³M. Bée, *Quasielastic Neutron Scattering* (Adam Hilger, 1988).
- ¹⁴Identification of a commercial product does not imply recommendation or endorsement by the National Institute of Standards and Technology, nor does it imply that the product is necessarily the best for the stated purpose.
- ¹⁵J. R. D. Copley and J. C. Cook, *Chem. Phys.* **292**, 477 (2003).
- ¹⁶R. T. Aзуаh, L. R. Kneller, Y. Qiu, P. L. W. Tregenna-Piggott, C. M. Brown, J. R. D. Copley, and R. M. Dimeo, *J. Res. Natl. Inst. Stand. Technol.* **114**, 341 (2009).
- ¹⁷B. Hess, C. Kutzner, D. van der Spoel, and E. Lindahl, *J. Chem. Theory Comput.* **4**, 435 (2008).
- ¹⁸W. L. Jorgensen, D. S. Maxwell, and J. Tirado-Rives, *J. Am. Chem. Soc.* **118**, 11225 (1996).
- ¹⁹M. P. Allen and D. J. Tildesley, *Computer Simulation of Liquids* (Oxford University Press, 1987).
- ²⁰A. Sahoo, S. Sarkar, P. S. Krishna, and R. N. Joarder, *Pramana* **63**, 183 (2004).
- ²¹A. H. Narten and A. Habenschuss, *J. Chem. Phys.* **80**, 3387 (1984).
- ²²S. Sarkar and R. N. Joarder, *J. Chem. Phys.* **99**, 2032 (1993).
- ²³T. Yamaguchi, K. Hidaka, and A. Soper, *Mol. Phys.* **96**, 1159 (1999).
- ²⁴A. Adya, L. Bianchi, and C. Wormald, *J. Chem. Phys.* **112**, 4231 (2000).
- ²⁵A. Karmakar, P. Krishna, and R. Joarder, *Phys. Lett. A* **253**, 207 (1999).
- ²⁶F. J. Bermejo, F. Batallán, E. Enciso, A. J. Dianoux, and W. S. Howells, *J. Phys.: Condens. Matter* **2**, 1301 (1990).
- ²⁷P. N. Pusey, H. N. W. Lekkerkerker, E. G. D. Cohen, and I. M. de Schepper, *Physica A* **164**, 12 (1990).
- ²⁸M. Hendrix, A. Leipertz, M. Fiebig, and G. Simonsohn, *Int. J. Heat Mass Transfer* **30**, 333 (1987).
- ²⁹T. R. Kirkpatrick, *Phys. Rev. A* **32**, 3130 (1985).
- ³⁰A. Faraone, K. Hong, L. R. Kneller, M. Ohl, and J. R. D. Copley, *J. Chem. Phys.* **136**, 104502 (2012).
- ³¹P. Sillrén, A. Matic, M. Karlsson, M. Koza, M. Maccarini, P. Fouquet, M. Götz, T. Bauer, R. Gulich, P. Lunkenheimer, A. Loidl, J. Mattsson, C. Gainaru, E. Vynokur, S. Schildmann, S. Bauer, and R. Böhmer, *J. Chem. Phys.* **140**, 124501 (2014).